Hypersonic Boundary-Layer Transition with Ablation and Blowing*

Steven P. Schneider†
School of Aeronautics and Astronautics
Purdue University
West Lafayette, IN 47907-1282

Abstract

Hypersonic boundary-layer transition is affected by many factors, including Mach number, Reynolds number, geometry, roughness, and tunnel noise. The effect of ablation or surface blowing is reviewed by summarizing the experimental data. Blowing generally moves transition upstream, with larger massflow rates or lighter gases causing a larger effect. Blowing that occurs farther upstream on the model generally also has a larger effect. It may be feasible to estimate the effect of blowing using semi-empirical stability-based methods such as e^N. Experimental data suitable for comparisons to these methods are summarized, for blunt bodies and for slender bodies at zero and nonzero angles of attack.

Introduction

General

The following was developed primarily for analyzing boundary-layer transition on the Orion or CEV, a manned NASA reentry vehicle that is very similar to Apollo. Transition on the Crew Exploration Vehicle (CEV, or Orion) is likely to be dominated by the effects of ablation and the laminar-ablated roughness, both isolated and distributed. The present document reviews the effect of ablation and blowing on hypersonic transition.

The author has earlier reviewed transition on reentry capsules and planetary probes [1]. See also the other transition issues reviewed in Refs. [2, 3, 4]. An overall review of roughness effects on hypersonic transition was reported in Ref. [5]; the reader is referred there for a general introduction to the present paper, with more complete references. The effects of roughness on transition for high-speed blunt bodies were earlier reviewed in Ref. [6]. Although roughness and ablation effects are often coupled, an attempt has been made to cover them in separate papers to keep each paper to a manageable length.

Transition on blunt reentry vehicles is affected by the chemistry and massflow of the gases blown from the ablating thermal protection system (TPS). It is also affected by the surface roughness of the laminar ablated TPS. This is a complex problem which was comprehensively researched in the 1960's and 1970's, partly to support the development of nosetips for slender military reentry vehicles. However, the area then fell out of favor, little has been done since the 1980's, and few of the earlier researchers are still available for comment.

The author has worked almost exclusively on transition since 1985, and on high-speed transition since 1990, but even an 8000-paper library and database is far from complete; the author still has much to learn about the vast literature for high-speed transition. The present review is focused on the effects of surface ablation and blowing. The review is limited to work that has appeared in the open literature. The author would appreciate hearing of errors and omissions.

The important of blowing or ablation to instability and transition has been known for more than 50 years. Morkovin reviewed it in 1969 [7, p. 66]. As Morkovin notes, a series of reports from the Naval Ordnance Laboratory developed methods of analyzing the stability of laminar boundary layers with blowing, during 1957-1967 [8, 9]. The first experimental data from the open literature dates from 1958 [10]. Morkovin also notes that the experimental data as of 1969 was inconclusive (for details, see citations below).

Physics of Instability and Transition with Blowing

Morkovin's review shows shadowgraph images taken from Pappas and Okuno [11]. Pappas and Okuno measured on a 7.5-deg. half-angle sharp cone in the NASA Ames 10-inch heat-transfer tunnel, us-

*AIAA-2008-3730, presented at the June 2008 AIAA Fluid Dynamics Meeting

†Professor. Associate Fellow, AIAA.

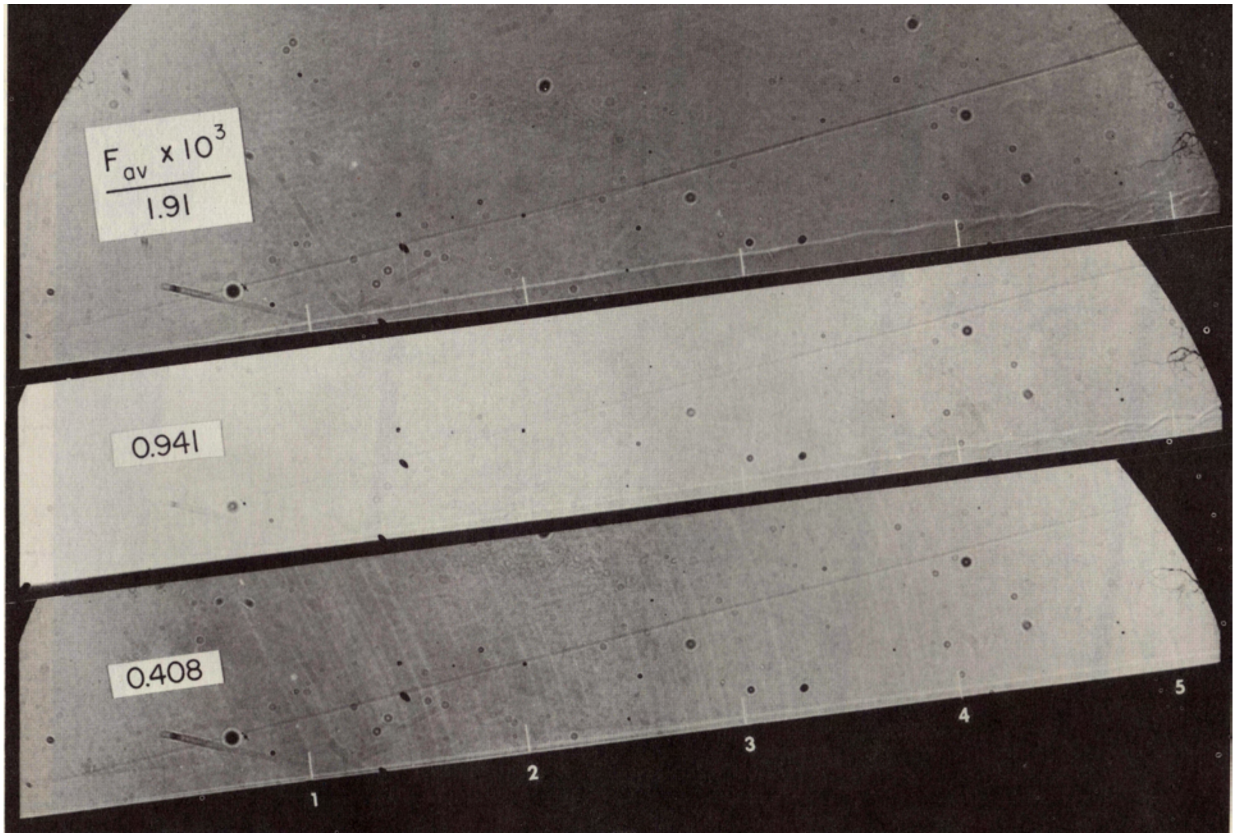

Figure 1: Shadowgraph of Instabilities with Air Blown into Air. From Ref. [11, Fig. 3b]

ing air, helium, and Freon-12. For all three experiments shown here, the edge Mach number was near 4.8 and the Reynolds number at the boundary-layer edge was about 2.3 million per foot. The slant length of the cone was 10 inches. The injection rate was measured along the cone, yielding average nondimensional rates of $F_{av} = (\rho_w v_w)/(\rho_c u_c)$, where ρ_w is the density of the blown gas at the cone surface, v_w is the velocity of the blown gas at the wall, normal to the cone surface, ρ_c is the inviscid freestream velocity at the cone surface, and ρ_c is the inviscid freestream density at the cone surface. Eight thermocouples were spaced 1.0 inches apart along a primary ray, beginning 1.0 inches from the start of the porous surface, and 2.2 inches from the tip of the cone. Three secondary rays each had 4 thermocouples, spaced 2 inches apart. The shadowgraphs were scanned into grayscale at 600 dpi from an original paper copy (no source of original photographs is known). The images are of considerable qualitative interest; however, Pappas and Okuno do not report any quantitative transition results, focusing instead on the laminar heat transfer.

Fig. 1 shows the shadowgraphs for air, at $F_{av} = 0.408 - 1.91 \times 10^{-3}$. The numbers shown in white letters on the black cone surface appear to be the numbers of the thermocouples. At the lowest blowing rate, the white line indicating the edge of the laminar boundary layer appears smooth and straight. At $F_{av} = 0.94 \times 10^{-3}$, some waviness is evident near the boundary-layer edge towards the end of the image. At the highest blowing rate, the flow appears turbulent at the downstream end of the image. The turbulent flow causes a visible outward displacement in the bow shock, beginning near thermocouple 2.

Fig. 2 shows the shadowgraphs for Freon-12, at $F_{av} = 0.519 - 2.00 \times 10^{-3}$. At the lowest two blowing rates, the flow again appears laminar at the downstream end of the image, and no waves are visible. At $F_{av} = 1.47 \times 10^{-3}$,, some waviness is just evident at the downstream end. At $F_{av} = 2.00 \times 10^{-3}$, waves are evident in the last quarter of the image, and the flow again appears turbulent at the downstream end. On the whole, the results are similar to air, with slightly less instability.

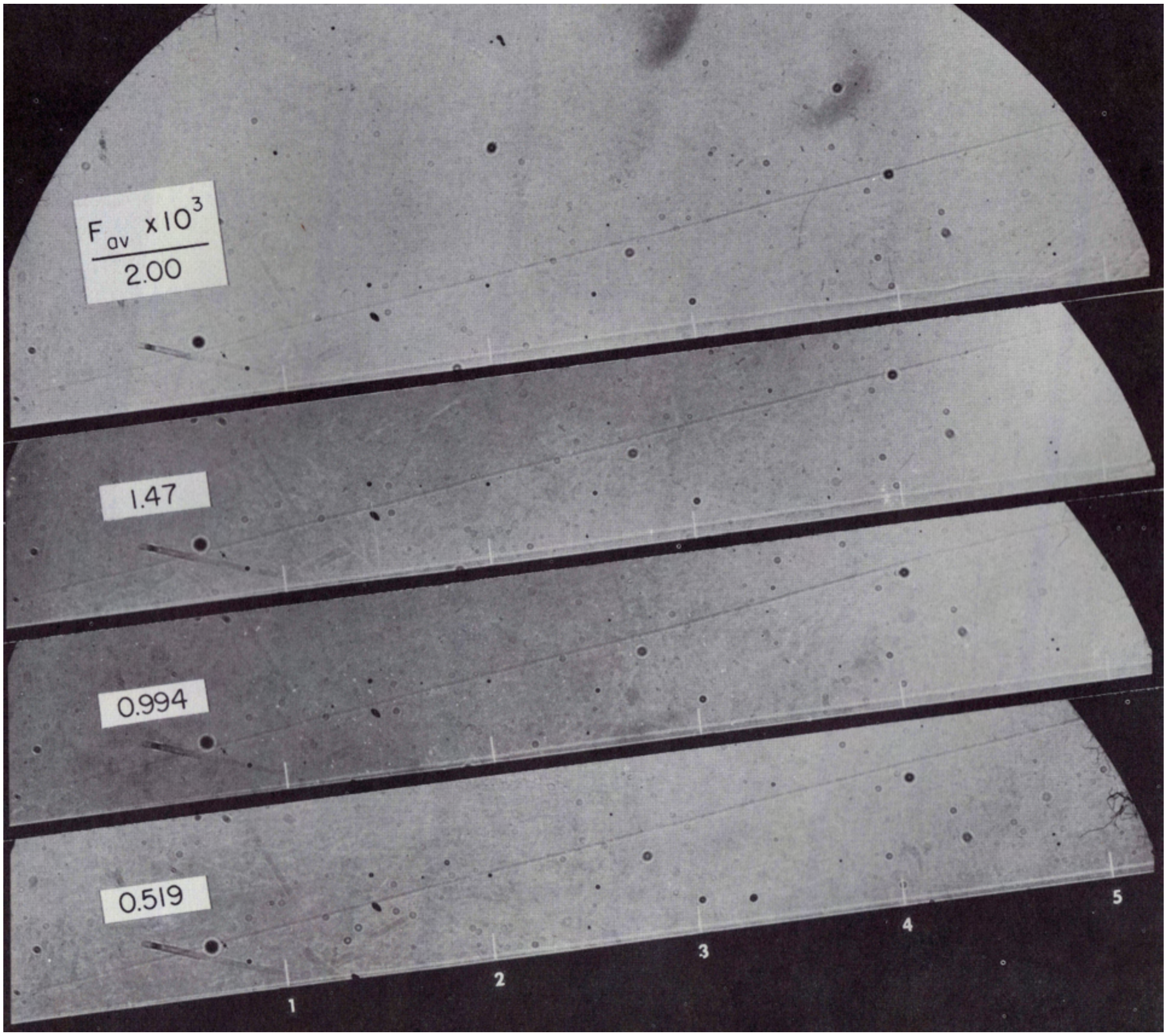

Figure 2: Shadowgraph of Instabilities with Freon-12 Blown into Air. From Ref. [11, Fig. 3c]

Fig. 3 shows the shadowgraphs for helium, at $F_{av} = 0.128 - 1.032 \times 10^{-3}$. Morkovin notes that helium blown at the same massflow rates has a much larger effect; he also notes that the large waves visible at the boundary-layer edge do not affect the heat transfer at the wall until well downstream. At the four largest massflow rates, the flow appears turbulent by the downstream end of the image. Detailed measurements are needed.

This Ames research focused on turbulent heating, so the transition data was produced as a byproduct [12]. Ref. [13] summarizes earlier measurements by Pappas which show the effect of surface blowing on transition. These 1958 results were later described in Ref. [14], which reports measurements on a 7.5-deg. half-angle cone at zero angle of attack in the NASA Ames 10-inch heat-transfer tunnel. The cone was apparently sharp, with fairly uniform blowing starting about 2 inches from the tip. The slant length to transition onset, x_T, was determined by the first appearance of turbulent eddies in shadowgraphs. Fig. 4 shows results at a cone edge Reynolds number of 5.25×10^6/ft. and an edge Mach number of 4.28. The lines are drawn only to aid the eye. Compared on a massflow basis, the light gas helium has the largest effect on transition, and the heavy gas Freon-12 the smallest. Increases in the blowing rate move transition forward, but transition never moves to the forward end of the blowing region. With zero blowing rate, all three curves should

Figure 3: Shadowgraph of Instabilities with Helium Blown into Air. From Ref. [11, Fig. 3d]

give the same result; the two curves with near-zero blowing points are pretty close. These early data are limited but suggestive.

The large waves that are particularly evident in Fig. 3 are reminiscent of the second-mode waves described in Ref. [15], and measured using hot wires and shadowgraphs. Demetriades performed experiments on a 5-deg. half-angle cone in AEDC Tunnel B at Mach 8 [15]. The cone was 5 ft. long and the freestream unit Reynolds number ranged from $1.7-2.6\times10^6$/ft. The porous cone permitted surface blowing, which was characterized using a nondimensional rate equivalent to F_{av} defined above.

Many details are omitted from this short paper. However, Fig. 5 shows shadowgraphs of waves near the boundary-layer edge which were clearly identified as second-mode waves, using hot-wire measurements and theoretical computations. Fig. 6 shows shadowgraphs with air blown through the porous cone, showing similar waves. *'The photographs showed that the waves were always present in the laminar boundary layer; it was common to find a wave train 10-20 wavelengths long upstream of transition.'*

Under small blowing rates, even at small angles of attack, the instability waves grow, become large enough to be evident in a shadowgraph, and then break down to transition. Higher blowing rates and apparently lighter gases both make the boundary layer more unstable, and cause earlier transition. Of course, this process depends on noise sources and the mechanisms of transition, so it depends on model geometry, Mach number, Reynolds number, angle of attack, freestream and model temperatures, and so on. Spatial and temporal nonuniformity in the blowing process will generate disturbances which also affect transition. The general process is very complex, and mostly unknown. However, one might expect that similar processes are taking place under other conditions when detailed measurements are not available.

Blowing on Blunt Geometries

McMahon 1958

McMahon carried out one of the earliest experiments with gas blown through a blunt body [16]. The 10-deg. half-angle cone had a nose radius of

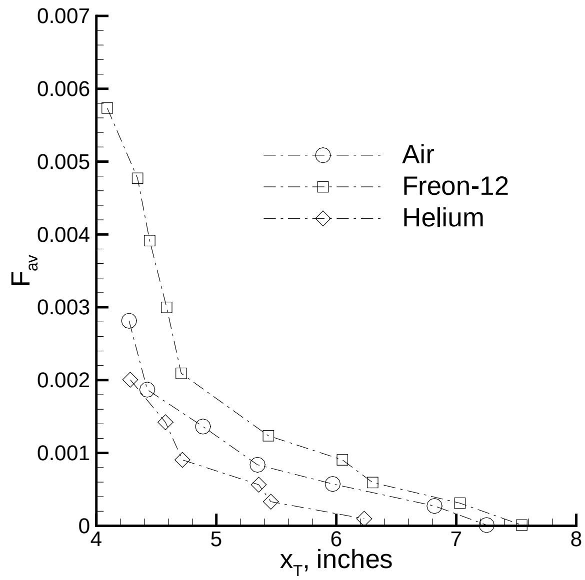

Figure 4: Variation of Transition Point with Injection. Sharp Cone at Zero Angle of Attack. Redrawn from Ref. [14, Fig. 4c]

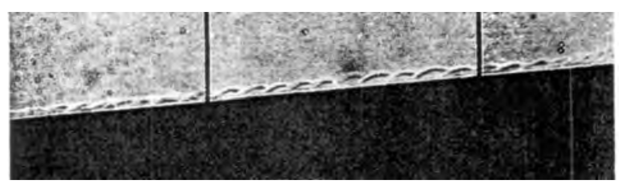

Figure 5: Shadowgraph of Second-Mode Instabilities on a Cone in Air. Zero Angle of Attack, No Blowing. From Ref. [15, Fig. 1a]

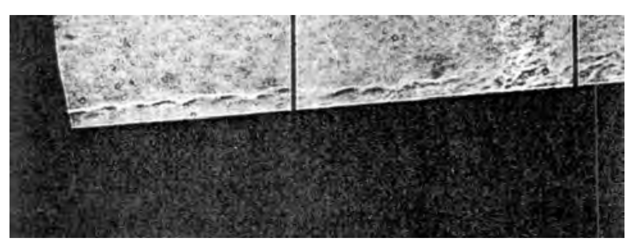

Figure 6: Shadowgraph of Second-Mode Instabilities on a Cone in Air. Zero Angle of Attack, Air Blowing at $F_{av} = 1.5 \times 10^{-3}$. From Ref. [15, Fig. 1b]

0.70 in. and a base radius of 0.875 in. The measurements were made at Mach 5.8 in the 5-inch tunnel at Caltech, at freestream Reynolds numbers of $0.95 - 2.43 \times 10^6$/ft. Helium and nitrogen were injected only through a small 0.063-in.-dia. hole at the stagnation point, so distributed ablation was not simulated. High rates of blowing were compared to the spiked-body case. Unfortunately, the limited measurements show no clear evidence of transition, which is not discussed.

Wilkins and Tauber 1966-1971

Wilkins and Tauber measured transition on 30-deg. half-angle plastic cones flown down a ballistic range at speeds to 7 km/s [17]. The base diameter was 1 cm and the local Reynolds numbers based on slant length ranged from $Re_x = 3 - 12 \times 10^6$ at freestream Mach numbers from 7 to 21. The cones were made from polycarbonate or polyformaldehyde, and were recovered after rapid deceleration in flight. Turbulent wedges were ablated into the recovered cones; these wedges apparently originated at small roughnesses on the model. In some cases laminar flow extended to a length Reynolds number of $Re_x \simeq 8\times10^6$. Ablation at 6.4 km/s was sufficient to remove 8% of the mass of a polyformaldehyde cone. Simple computations were made to predict the mass loss for laminar and turbulent flow, and the amount of mass ablated from a cone was compared to this analysis and a measurement of the fraction of the surface covered by turbulent wedges.

Wilkins continued this work for several years, reporting last in 1972 [18]. Cones with 30-deg. and 50-deg. half-angles were launched at 2-6 km/s. The base diameters were 1.0 and 1.2 cm. Most of these later cones were made from Delrin (nylon) but some were of polycarbonate and cellulose nitrate. Most cones were launched with sharp tips but some tips were blunted to as much as 9% of the base radius before launch. The axial distribution of surface recession was measured postflight and compared to theory in order to determine the location of transition.

Most of the 30-deg. half-angle cones experienced laminar flow, while most of the 50-deg. half-angle cones experienced turbulent flow. Earlier measurements at similar conditions were thought to be contaminated by tip damage that was avoided in later measurements. Although some turbulent flow was observed at $Re_x \simeq 1 - 2 \times 10^6$, significant laminar flow sometimes extended to $Re_x \simeq 14 \times 10^6$. Much of the variation in transition location was attributed to small roughness elements that were present at launch or developed during ablation in flight. Polycarbonate transitioned at about the same Reynolds numbers as Delrin, but cellulose nitrate transitioned much earlier. This work by Wilkins et al. is unusual and suggestive, but reliable interpretation would require new computations and experiments.

Demetriades et al. 1976

Demetriades et al. measured on a spherically-blunt 5-deg. half-angle cone with a 7-in. nose radius, in the 50-in. Mach-6 nozzle of AEDC Tunnel B [19]. The nose was made of porous sintered metal, with a thickness distribution designed to simulate the mass-flux distribution on an ablating RV. Air was injected at temperatures near the stagnation temperature, and $Re_D \simeq 3.9 - 6.2 \times 10^6$. Here, Re_D is a Reynolds number based on nosetip diameter and freestream conditions. Measurements were made with hot wires and small pitot probes. Transition was inferred from the fluctuations in the hot-wire signals and from changes in the mean flow profiles. The angular location of transition was correlated with Re_D and the blowing rate. Although these measurements are very interesting, and appear to be of high quality, this short two-page note does not provide enough information for a detailed reanalysis.

Feldhuhn 1976

Feldhuhn measured heat transfer on an RV nosetip at Mach 5 in a 16-inch tunnel at freestream unit Reynolds numbers of 3.8, 7.4, and 17.8 million per foot [20]. The 5-deg. half-angle sphere-cone had a 2-in. nose radius (R_n) and was 15 in. long. Three separate chambers were designed to blow coolant through porous regions from $0 < s/R_n < 0.52, 0.52 < s/R_n < 1.48$, and $1.48 < s/R_n < 3.24$. Here, s is the arc length from the stagnation point. The aft cone was impermeable. The model was instrumented with 20 thermocouples. Coolant flow rates varied up to about 1% of the freestream massflow per unit area. Transition was inferred when the heat transfer rose above values computed by a boundary-layer code. Feldhuhn's Case 35 showed that blowing on the nosetip of $\rho_w v_w/(\rho_\infty u_\infty) = 0.007$ could cause transition near $S/R_n = 0.5$, at $Re_\infty = 3.9 \times 10^6$/ft. Here, $\rho_\infty u_\infty$ is the freestream massflow per unit area. It would be interesting to compare the results to a modern computation. Unfortunately, the NSWC report listed in Feldhuhn's references was never completed. Although the AIAA paper contains the only experimental description which remains available (Robert Feldhuhn, private communication, May 2008), it may still be sufficient to enable such a comparison.

Williams et al. 1976

Williams et al. measured transition on a reentry-vehicle (RV) nosetip during ablation in an arcjet [21]. The measurements were made in the High Impact Pressure arcjet at the McDonnell-Douglas Research Laboratory. The Mach number was 1.7 and the stagnation pressure ranged from about 10 to 100 atm., for a freestream unit Reynolds number of $5-15\times10^6$/ft. The hemisphere-cylinder models had a nose radius of 0.15 inches. High-speed cameras were used to image the model, and a pyrometer measured the surface temperature. As the plenum pressure was ramped from about 15 to 120 atm. over about 5 s., the nosetip ablated. Laminar, transitional, and turbulent flow were inferred from ablation rates and the average surface temperature. Transition onset occured at a sonic-point unit Reynolds number of about $6-8\times10^6$/ft. This corresponds to a Reynolds number based on nosetip diameter of less than 100,000, perhaps because of the high noise levels in the arc jet. A carbon/carbon nosetip transitioned later than the nominally smoother ATJ-S graphite nosetip, perhaps because of a flaw in the graphite sample (cp. Ref. [22]). Although this report suggests an interesting and useful capability, the results presented are insufficient for detailed analysis.

Kaattari 1978

Kaattari measured heat transfer on three blunt models in the NASA Ames 3.5-ft tunnel at Mach 7.3, with air blown through porous surfaces [23]. Kaattari focused on high blowing rates anticipated for entry to outer planets, but also obtained data at low blowing rates. The models were made from 6.35-mm-thick porous stainless steel, 17.78 cm. in dia., in the form of a hemisphere, a 30-deg. half-angle blunt cone with a 1.91-cm nose radius, and a 21.34-cm-radius spherical segment. Each model included 5 pressure taps and 16 slug calorimeters. The porosity was nearly uniform, and the distribution of massflow was measured and tabulated. The Reynolds number based on freestream conditions and model diameter, Re_D, ranged from 0.6 to 5.2 million. Under laminar flow, the heating decreased with arclength s; transition was inferred when the heating rates suddenly increased.

For the hemispherical model at $Re_D \simeq 1.1\times10^6$, laminar flow was observed for $\lambda_\infty = \rho_w v_w/(\rho_\infty u_\infty) = 0.003$ and 0.007, as shown in Fig. 7. Here, q is the local heat transfer coefficient, and q_0 is the stagnation point value on the hemispherical model without blowing. When the blowing rate increased to $\lambda_\infty = 0.022$, transition began at about $s/R_n = 0.28$, moving slightly upstream to near $s/R_n = 0.2$ for $\lambda_\infty \geq 0.027$ (data for higher blowing rates are not shown). For the hemispherical model at $Re_D \simeq 2.3\times10^6$, laminar flow was observed for $\lambda_\infty = 0.004$. When blowing increased to $\lambda_\infty = 0.010$, transition began at about $s/R_n = 0.9$, moving forward to $s/R_n \simeq 0.7$ when $\lambda_\infty = 0.013$. For $\lambda_\infty \geq 0.016$, transition stayed near $s/R_n = 0.2$. Transition also occurred on the other two models, although the data are less clear.

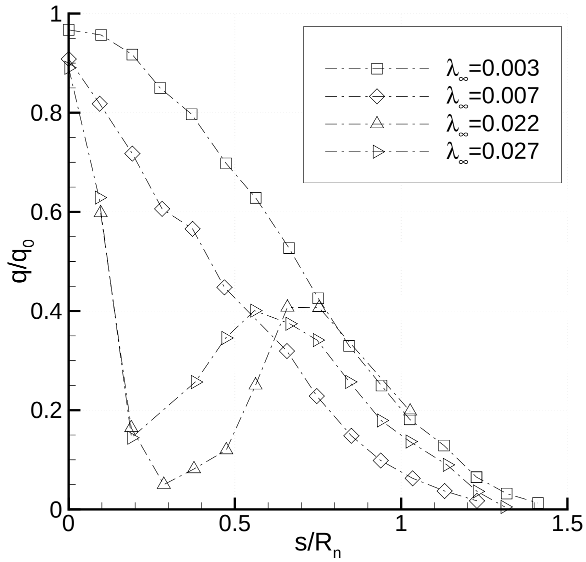

Figure 7: Heat-Transfer Distribution on a Porous Hemisphere in Air. Redrawn from Ref. [23, Fig. 4a]

Kaattari's data appear to be of good quality, with considerable detail recorded in the 64-page report. As stability-based transition-estimation techniques become available for blunt bodies with blowing, the present author suggests beginning with comparisons to this hemisphere data.

Other Measurements and Computations

Winkler et al. studied arcjet flow within an axisymmetric duct of ablating teflon [24]. The pressure gradient was nearly zero. The ablation rate decreased downstream of the duct entrance, presumably because the thickening laminar boundary layer produced less heat transfer. Farther downstream, the ablation rate suddenly increased, presumably due to transition to turbulence on the duct walls. Yet farther downstream, the ablation rate decreased again, presumably due to the thickening of the turbulent boundary layer. At transition onset, the momentum thickness Reynolds number was about 450 and the edge Mach number was about 3. Streamwise vortices apparently formed near the transition location.

Winkler's apparatus suggests a different and possibly useful method of measuring ablation-induced transition. The very limited results might also be compared to a modern computation, although arcjet flows are known to have a high level of noise and contamination.

Baker reviews ablation and transition on blunt RV nosetips, in the course of developing computational approaches [25]. However, the location of transition is taken from simple correlations, since the focus of the paper is on the simulation and on roughness-augmented turbulent heating. Baker points out that the roughness on an actual nosetip in flight is very uncertain.

Park developed theory and computations for turbulent heating induced by ablation-induced mass injection [26]. He suggests that a nominal time constant for the fluctuations in ablation is about 2×10^{-4} s. Although Park's paper contains useful references and interesting discussions of the fluctuations induced by ablation, it does not bear directly on the issue of transition.

Yamada et al. measured the heat flux to a capsule-shaped body with mass injection, in a shock tunnel near Mach 10 [27]. The freestream Reynolds number ranged from $0.8 - 2.4 \times 10^6$/m. The 45-deg. half-angle blunt-cone model had a base diameter of 0.16 m and a nose radius of 50 mm. Transition was inferred from infrared-camera measurements of heat transfer. Transition appears to occur for $\lambda_\infty \simeq 0.02 - 0.03$ when the arclength Reynolds number is about 3×10^4 and $Re_D \simeq 0.25 \times 10^6$. However, the data are limited and some of the description is difficult to interpret.

Blowing on Slender Non-Lifting Geometries

Scott 1958-1960

Scott measured transition on a 8.0-deg. half-angle cone at Mach 5 in the 6x9-in. continuous-flow tunnel at the Rosemount Aeronautical Laboratories of the University of Minnesota [28]. The tunnel used more than 5000HP, and was closed long ago. The cone was 14.7 in. long with a solid steel tip that was 1 in. long. Nitrogen and helium were blown through the sintered-stainless-steel frustum, and the axial distribution of blowing was carefully measured. Transition onset was measured using shadowgraphs. Most of the measurements were made at a freestream unit Reynolds number of 4.6 million per foot, which was reported to be sufficient to permit obtaining good shadowgraphs, although transition did not extend to the rear of the model.

When nitrogen was blown at a wall-to-total temperature ratio of $T_w/T_0 \simeq 0.65$, the arclength transition Reynolds number decreased from about 3-4 million to about 2 million as the blowing rate increased from zero. When $T_w/T_0 \simeq 0.8$, the transition Reynolds number was consistently lower by perhaps 10-20%. When helium was blown, the transition Reynolds number decreased from about 3-4 million to about 1 million as the blowing rate increased from zero, with a somewhat higher transition Reynolds number at low blowing rates for colder walls.

Since the blowing rates are given in terms of a complex parameter, further analysis would be needed to compare the results to the other experiments. The data are not tabulated and the copy of the report that is furnished by DTIC is only marginally readable. The Univ. of Minnesota still has the original copies of these reports (private communication, Bailey Diers, U.M. Archives, Elmer L. Andersen Library, 13 June 2008).

An earlier report on these measurements still has limited distribution, but was summarized in Ref. [10]. Injection of air and helium both moved transition forward by as much as 30%, with less helium being required to produce the effect. A complex parameter was again used to nondimensionalize the mass injection rate. The results appear to be consistent with Pappas; blowing moves transition upstream, and lighter gases have a larger effect for the same massflow.

Dunavant and Everhart 1969

Dunavant and Everhart measured on a 3.75-deg. half-angle cone in the 31-in. Mach-10 tunnel at NASA Langley [29]. The cone was 69.38 in. long. It included a short porous section between 3.80 and 7.30 in. through which both air and helium were blown through a surface area of 7.13 sq. in. The model included 21 pressure taps and 116 thermocouples, from which heat-transfer and transition were inferred. The freestream unit Reynolds number varied from 0.47 to 1.75 million per foot and the tunnel stagnation temperature was typically 1028K.

The model was precooled to a nonuniform wall temperature of 0.2-0.5 of the stagnation temperature.

Mass injection rates varied from 0.0003 to 0.0084 times the flow rate through a stream tube equal to the base area (64.94 sq. in.). These rates were large for a relatively small area, and caused the pressure over the porous section to reach 2-5 times the value without blowing. The higher pressures occured for helium blowing. The effect on transition of this large axial pressure gradient is unknown.

Transition was inferred when the streamwise distribution of heat transfer rose significantly above the slope of the laminar theory. However, the inferred transition locations are subject to interpretation. Mass injection lowers heating due to the film cooling effect, which was not accurately computed, and the heat-transfer distributions do not have a simple form. Transition onset seems to have moved well forward, perhaps all the way to the porous section, even for the lowest air blowing rate of 0.0011 at a length Reynolds number of 2.84 million. The helium heat-transfer data is even more difficult to interpret; although Dunavant and Everhart believe that helium blowing did not move transition forward, the data can also be used to infer that transition moved just as far forward as it did with air.

These measurements use a short mass-injection region which does not model ablation for a typical vehicle. In addition, the heat-transfer data are difficult to interpret, and the wall-temperature distribution is very nonuniform. It will be difficult to draw reliable conclusions regarding transition from these data. It would also be difficult to compare the experiments to modern computations.

Mateer and Larson 1969

Mateer and Larson inferred transition on a 5-deg. half-angle cone in the 3.5-ft. Mach-7.4 tunnel at NASA Ames using measurements of ablation [30]. The sharp steel nosetip was 2.5 in. long, followed by a 0.5-in.-long boron nitride insulator, and a 25-in.-long camphor frustum. The mass injection rate $\dot{m}/(\rho_\infty u_\infty A_B) = 0.007 - 0.04$, where $\dot{m}$ is apparently the total massflow due to ablation, ρ_∞ is the freestream density, u_∞ is the freestream velocity, and A_B is the base area of the cone. Measurements were also made with oversized nosetips and typical aft-facing steps to a metal frustum. Neither the camphor ablation nor the small aft-facing steps had a significant effect on the location of transition, perhaps because the camphor ablates gases of high molecular weight, and the aft-facing steps were small.

DiCristina 1970

DiCristina made measurements on non-ablating cones at zero and non-zero angle of attack in AEDC Tunnel C at Mach 10 [31]. The sharp cones had a 8-deg. half angle and a 10-in. base diameter. The tunnel was operated at freestream unit Reynolds numbers of 1.5×10^6/ft and 2.1×10^6/ft, with a total temperature of $1900°R$. Transition was measured with a spark shadowgraph. Ablation was studied using a low-temperature ablator formed from paradichlorobenzene, with few details being presented in the open literature. Low-frequency model oscillations had a quasi-steady effect.

DiCristina's Fig. 16 shows transition moving about 10-40% upstream when surface blowing increases from zero to $\dot{m}/(\rho_\infty u_\infty A_B) = 0.012$, depending on angle of attack. Here, $\dot{m}$ is apparently the total massflow due to ablation, ρ_∞ is the freestream density, u_∞ is the freestream velocity, and A_B is the base area of the cone. A detailed analysis would be necessary to compare these results to others, since the results are reported with a different scaling. Unfortunately, this short paper contains few details, and additional details are not available in the open literature.

Fischer 1970

Fischer measured transition on ablating and non-ablating 10-deg. half-angle cones at Mach 7 in the 11-in. tunnel at NASA Langley [32]. The non-ablating measurements were previously reviewed in Ref. [4]. The ablating measurements used a sharp stainless-steel nosetip following by a nylon insulator and a frustum of paradichlorobenzene that extended from 2.78 to 12.0 inches downstream of the tip. The onset of transition was determined using measurements of the surface recession vs. streamwise distance. The ratio of wall to total temperature was about 0.46.

Transition moved forward by 28-35% for the ablating cones with massflow rates of $\dot{m} = 0.0041$ to 0.0063, where $\dot{m}$ is total massflow divided by the freestream massflow per unit area and the cross-sectional area of the cone at the location where transition starts. An aft-facing step formed at the end of the stainless-steel nosetip, leading to streamwise grooves in the ablator. In a short summary, Fischer cites previous experimental data to argue that this step was probably too small to affect the results [33]. The spacing of the streamwise grooves was somewhat larger than that measured by Ginoux [34]. Fischer compared his ablation results to DiCristina, noting that ablation moved transition farther forwards in Fischer's experiments at a lower massflow rate, for unknown reasons [33].

It would be interesting to reanalyze the data using modern computations. Information on the reacting air chemistry of paradichlorobenzene might not be easy to obtain, although the chemical is still commonly available. Fischer's appendix provides details on the method of fabricating the ablating frustum.

Marvin et al. 1970

Marvin and Akin measured transition on a 5-deg. half-angle cone in the NASA Ames 3.5-ft tunnel at Mach 7.4 [35]. The sharp and blunt nosetips were about 3 in. long and impermeable. The blunt tips had nose radii of 1/32, 1/16, and 1/8 in. Argon, air, and helium were injected through a uniformly porous frustum that was about 16 in. long. The Reynolds numbers based on cone length and freestream conditions were 3, 4.7, and 7.8 million. Transition was inferred from heat-transfer measurements using thermocouples in the thin porous skin.

Fig. 8 shows results for air injection for a sharp cone. Here, $F_{av2} = \dot{m}/(\rho_\infty u_\infty A_B)$, with the symbols defined as for DiCristina above. Again, q is the local heat-transfer rate, $q_{s=1}$ is the heat-transfer rate at the beginning of the porous region, $s = x/L$ is the dimensionless arclength from the nosetip, and L is the arclength along the solid nosetip. A finite-difference boundary-layer code that included injection effects gave good agreement (not shown here) for the laminar heat transfer, which decreased monotonically with streamwise distance. Transition onset was inferred when the heating rate began to rise; at $s \simeq 4.4$ without blowing, at $s \simeq 3$ for $F_{av2} = 0.45$, at $s \simeq 2.9$ for $F_{av2} = 0.91$, and at $s \simeq 2.0$ for $F_{av2} = 1.60$. For the two highest blowing rates, the end of transition may be inferred when the heating rate peaks and begins to decline again as the turbulent boundary layer thickens downstream. Transition moves upstream with increased blowing rates.

Fig. 9 shows results for the lowest nonzero blowing rate for a sharp cone, for all three gases. Transition onset is earliest for the heaviest gas, argon, a bit later for air, and latest for the light gas, helium. Fig. 10 shows similar results for the next higher blowing rate. In this case, helium transitions earlier than the others, followed by argon and then air. Marvin and Akin argued that for a given rate of mass addition, the data generally show that transition moves furthest forward for the lightest gas. However, their data show that the effect of molecular weight may be different for different average blowing rates; at present there is no theoretical reason

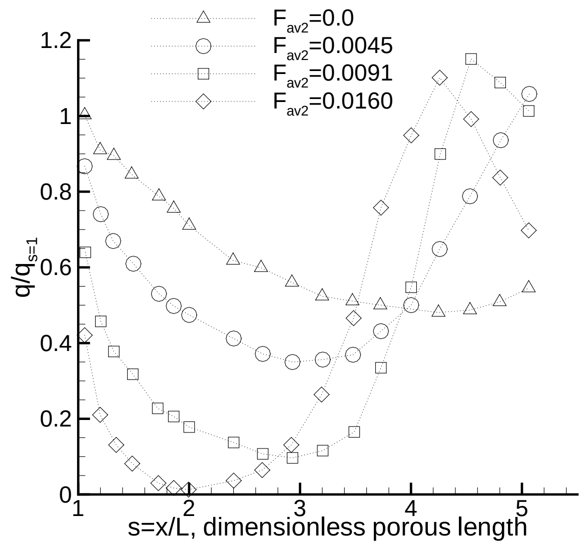

Figure 8: Effects of Air Injection on Heat Transfer to a Sharp Cone. From Ref. [35, Fig. 7a]

why this may not hold true. They present various correlations for the transition location.

Bluntness delayed transition, which still occurred if the blowing rate was high enough. Although the paper is fairly short, the description is reasonably complete, and the data appear to justify a modern reanalysis. Unfortunately, reports with further detail are not available (Joseph Marvin, private communication, May 2008).

Wimberly et al. 1970

Wimberly et al. measured transpiration and film-cooling effects on a 7.25-deg. half-angle cone in the Vought hotshot tunnel. Conical nozzles with a 13-in. exit diameter provided Mach 12 and 17 [36]. The model was 7.770 in. long with a 2.015-in. base diameter and a 0.017-in. nose radius. Methane was injected through two forward compartments on the model, while ethylene was injected through two aft compartments. Forces and moments were measured along with six thermocouples.

The measurements at Mach 17 and a freestream Reynolds number of about 1 million per foot were apparently all laminar. At Mach 12 and about 6-8 million per foot, mass injection moved transition upstream, as inferred from the heat transfer and drag data. However, the measurements are very limited,

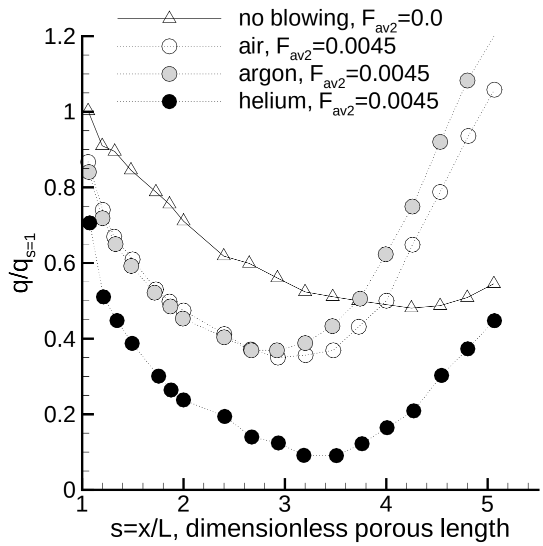

Figure 9: Effects of Low Injection Rates on Heat Transfer to a Sharp Cone. Replotted from Ref. [35, Fig. 7]

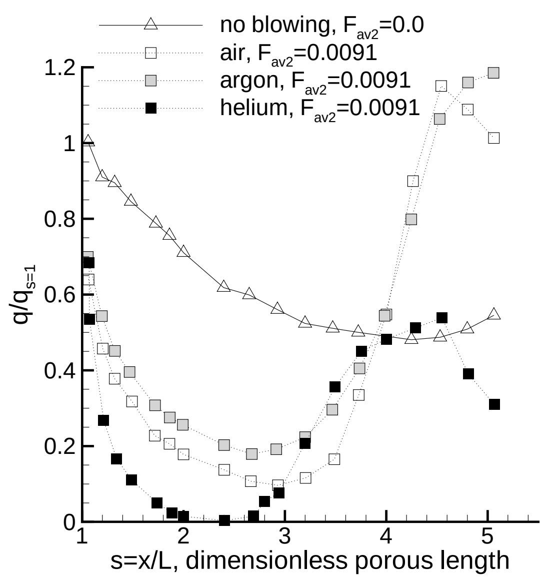

Figure 10: Effects of Higher Injection Rates on Heat Transfer to a Sharp Cone. Replotted from Ref. [35, Fig. 7]

and unlikely to be useful for comparisons to modern computations.

Stalmach et al. 1971

Stalmach et al. measured transition mostly on 12-deg. half-angle cones in the Vought hotshot tunnel near Mach 12 [37]. The conical nozzle generated a surface pressure that fell about 20% over the length of the cone. The sharp solid nosetip had a slant length of 0.381 in., about 4% of the overall 9.687-in. slant length. The nose radius is evidently small but was apparently not measured. The freestream Reynolds number varied from about 3-8 million per foot. Five runs were made with a 5-deg. half-angle solid cone.

Different porous cone experiments provided two measured blowing-rate distributions, one that was nearly uniform, and one that varied nearly as the square root of the arclength. The three gases injected were nitrogen, methane, and Freon. Transition was inferred from shadowgraphs and from measurements using 20 thermocouples placed along a primary ray with three more along a secondary ray. The heat-transfer rates were compared to a boundary-layer computation, which generally agreed well when the flow was laminar. The onset of transition was taken where the heat-transfer rate first rose from the laminar values. The end of transition was taken from the local heat-transfer maximum, or from the beginning of full turbulence in the shadowgraphs; these two indications generally agreed well. Turbulent bursts were observed in the spark shadowgraphs; these were usually between the onset and end of transition, although such bursts were sometimes observed upstream of the nominal onset of transition. The transition locations are tabulated for all 53 runs at 32 conditions including six with a screen-overlay roughness and seven that were completely laminar.

Mass injection reduced the heat transfer within the laminar boundary layer, in good agreement with the nonreacting computations. Both increasing massflow and decreasing molecular weight reduced the laminar heat transfer and also moved transition upstream. Transition moved upstream by as much as a factor of 2. The nonuniform injection distribution with more mass injected near the nose had a greater effect on transition than the uniform distribution did, for the same total massflow. The distance between the onset and end of transition was roughly equal to the distance from the nosetip to onset, with considerable scatter, and no obvious trend with injection rate or material.

The experimental conditions and results were carefully reported. Although the conical nozzle produced a favorable pressure gradient, it was carefully documented and might be taken into account in a modern stability-based reanalysis. Hot-shot tunnels are known to produce higher levels of freestream noise, and the results were not compared to Pate's correlation to determine if this noise was of the usual sort. However, the injected mass was varied while the tunnel conditions were kept nearly constant, so the tunnel noise should be nearly constant and it would seem possible to isolate the effect of injection rate on the integrated growth of instabilities.

Martellucci 1972

Martellucci measured boundary layer properties on a 7.25-deg. half-angle sharp cone at Mach 8 in AEDC Tunnel B [38, 39]. The nose was impervious, but air was blown through a porous frustum downstream of $0.19L$, where the cone length $L = 41.66$ in. Transition was inferred from impact pressures obtained by traversing a pitot probe along the surface. At a freestream unit Reynolds number of 2.7 million per foot, and zero angle of attack, the onset of transition moved upstream from about $0.4L$ for zero blowing to near $0.3L$ for $\dot{m} = 0.01$, where $\dot{m}$ is the total blowing massflow divided by the freestream massflow per unit area and the model base area. For larger massflows of $\dot{m} = 0.025$ and 0.05, Martellucci reports transition moves aft to a bit more than $0.4L$ and then about $0.45L$. Martellucci argues that at low blowing rates, the blown air destabilizes the boundary layer, whereas at higher blowing rates, the wall cooling due to blowing overwhelms this effect, stabilizes the boundary layer, and moves it aft again.

A few more details are available in Ref. [40], but since the work was focused on turbulent boundary layers the transition data is very limited. The downstream movement of transition for higher blowing rates is very surprising and must be viewed skeptically unless it can be supported by additional information. It seems possible that there is some error in the inferences from the surface impact pressures.

Starkenberg, Plostins, and Cresci 1976-1982

Starkenberg and Cresci measured film-cooling and transition on a 10-deg. half-angle cone in the 2-ft.-dia. Mach-8 blowdown tunnel at the Polytechnic Institute of New York [41]. The model had a 0.5-in.-radius nose made partly from sintered stainless steel. Air was blown through the tip of the nose, through the region upstream of 30 deg. from the stag. point. The stagnation temperature was about $2000°R$ and the unit Reynolds number varied from 0.12 to 0.96 million per foot. The length of the cone is not stated, but appears to be slightly greater than 25 inches. Heat transfer rates are inferred from thermocouples on a thin-skin model. Transition is inferred by comparing the heat transfer to a boundary-layer computation.

As the blowing rate increases for a fixed unit Reynolds number, transition occurs on the back of the model and then moves upstream. For higher values of the blowing rate, at lower unit Reynolds numbers, transition appears to occur near the nosetip, after which the flow appears to relaminarize, and then transition again downstream.

It would be interesting to compare the results to a modern computation. Although most results are given in a complex nondimensional form, it seems possible to infer the basic conditions. The symbols s and $\bar{s}$ are used but never clearly defined in Ref. [41]. However, p. 9 of Ref. [42] states that $\bar{s}$ is the distance from the stagnation point divided by the nose radius. Starkenberg's Ph.D. thesis probably provides additional information. The present author is skeptical about the streamwise relaminarization that is inferred by comparing heat transfer to the film-cooling boundary layer code. It appears that similar skepticism existed at the time, for hot-film measurements were later performed in the same facility to clarify this issue [42]. In combination with the work of Martellucci and others, these measurements might shed light on the effect of nosetip ablation on frustum transition.

Plostins and Cresci carried on the work of Starkenberg and Cresci [41] by measuring with a single flush-mounted hot-film in the same tunnel [42]. Freestream unit Reynolds numbers varied from 0.14 to 1.6 million per foot, at a total temperature of $2000°R$. Plostins fabricated a 10-deg. half-angle cone with a 1.1-in. nose radius that was 12.3 in. long; the model again included a porous nose section that permitted blowing in a region up to 30-deg. from the tip. He also carried out additional measurements using Starkenberg's cone.

The onset of transition was inferred from an increase in the uncalibrated RMS fluctuations on the hot film; this location apparently agreed fairly well with the Starkenberg's inference from heat transfer. Transition was correlated for a variety of unit Reynolds numbers using two parameters: 1) a scaled arclength times the momentum-thickness Reynolds number at transition onset divided by the square root of the freestream Reynolds number, and (2) a scaled blowing rate multiplied by a scaled arclength.

Although it would be interesting to compare the results to a modern computation, the basic hot-film results at zero angle of attack are not given in a form which permits reanalysis. The effect of angle of attack on transition induced by nosetip blowing is given for a hot-film located 9.09 nose radii downstream.

Ref [43] provides additional detail regarding the heat-transfer measurements including results at angle of attack. The heat-transfer data are plotted in a form which appears to permit reanalysis. The relaminarization inferred from both the heat transfer and the hot-film fluctuations does seem to be reasonably well supported although it is very surprising. Further analysis with modern methods would be desirable.

<u>Boudreau 1977-1985</u>

Boudreau measured transition on a 9.75-deg. half-angle cone at Mach 7 in AEDC Tunnel F [44, 45]. The cone had a base radius of 4.4 in. and a large nose radius of 2.2 in. Coaxial surface thermocouples were used to measure heat transfer, from which transition was inferred. There were 48 thermocouples on the frustum and 11 on the nosetip, along four azimuthal rays. Measurements were made at initial unit Reynolds numbers of 10, 20, and 40 million per foot; these fell during the 50-200 ms runs as the hotshot tunnel blew down. The stagnation temperature ranged from $1000 - 1400°R$ while the model temperature was near $540°R$. The front half of the model formed one blowing chamber and the rear half formed a second. Small leaks around the sensors were plugged with cement that generated some roughness. The residual leaks may have had some effect on transition for this and other experiments, Boudreau believes. Nitrogen was blown through the forward chamber at rates near 0, 0.004, 0.008, and 0.04 lb./sec, and through the aft chamber at rates near 0, 0.001, 0.002, and 0.004 lb./sec. Nondimensional blowing rates are not given. The results are compared to laminar and turbulent computations.

With no blowing, the boundary layer is laminar at 3.1 million per foot, and apparently turbulent at 7.6 million per foot (Boudreau's Fig. 2). In the apparently turbulent case, the heating on the nosetip is still below the computation, especially near the shoulder, perhaps because the flow is not really turbulent until it reaches the frustum. Most figures show the heating vs. unit Reynolds number at a fixed station; these are more difficult to interpret, and involve implicit variations in tunnel noise. Nose section blowing rates of up to 0.002 lb/sec. had little effect on transition, with 0.008 lb/sec. moving transition forward by about 20% at the shoulder, and 0.04 lb/sec. moving transition forward by about a factor of two in unit Reynolds number. The AEDC report is very similar to the AIAA paper and does not contain tabulated data. Fig. 5 in Ref. [44] appears to show windside-forward transition for the cone with no blowing at 2-deg AOA.

This is an interesting experiment using a large cone with a large nose radius. The effect of nose blowing was measured in detail. However, the results are presented only in a summary fashion which would be difficult to reanalyze using modern computations.

<u>Yanta et al. 1989</u>

Yanta et al. measured on a 8-deg. half-angle porous cone at Mach 2.5 [46]. Although the detailed profile measurements are all for turbulent boundary layers, the description of the design and testing of blowing models might be useful.

Blowing on Lifting Geometries

Most experiments that studied the effect on transition of ablation or blowing have been carried out with symmetrical models. However, a few experiments have used lifting models.

<u>Morkovin and Donohoe 1967</u>

Morkovin and Donohoe measured the effects of blowing on a very blunt lifting shape with a control flap [47]. The measurements were performed in the 3.5-foot hypersonic tunnel at NASA Ames. The report gives a three-view drawing of the very blunt lifting body that was studied, but does not give the coordinates or otherwise fully specify the geometry. The nose radius is roughly 50% of the base radius, and a large body flap extends across much of the lower surface. The body was made of porous sintered metal, through which nitrogen was blown at various rates and at various temperatures; a good description of the blowing technology is given. Measurements were made using a shadowgraph, three pressure sensors on the lower surface, a six-component balance, two thermocouples, and two calorimeters. The freestream unit Reynolds number was 1.5 million per foot, the model was about 10 cm long and 7 cm wide, angles of attack were varied from 0 to 20 deg., and $\dot{m}$ varied up to about 0.01. Here, $\dot{m}$ is the ratio of the rate of mass injection to the product of the freestream velocity, freestream density, and body base area. The Reynolds number based on model length was about 0.48 million.

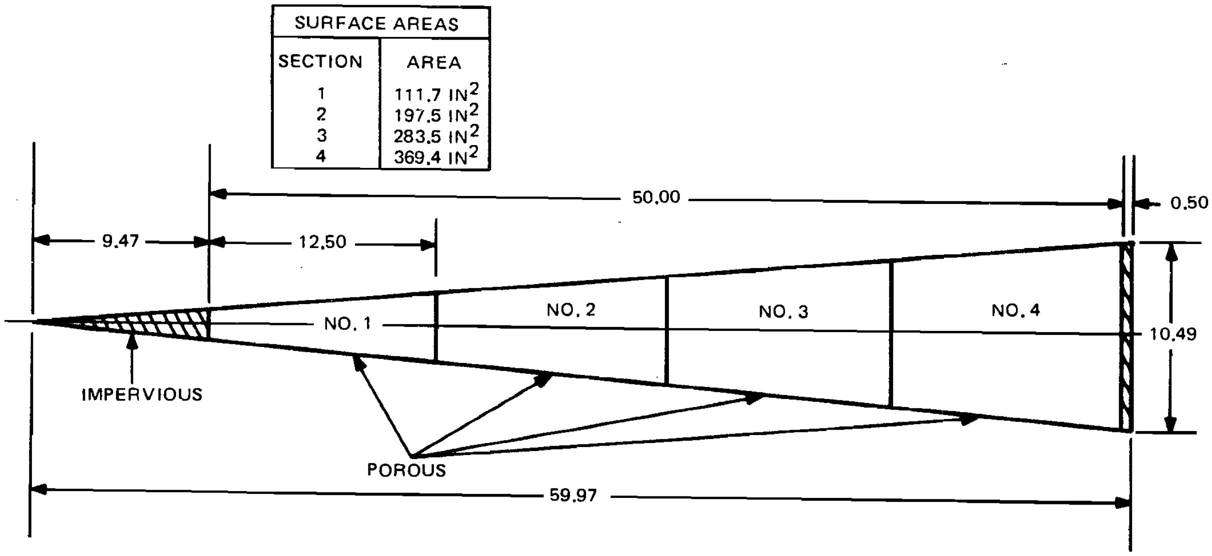

Figure 11: Schematic of Cone with Four Blowing Chambers. Dimensions in Inches. From Ref. [48, Fig. 1]

The report is focused on the three-dimensional separation induced upstream of the body flap, and its effect on control authority. Transition is inferred from shadowgraph images. The image quality in electronic files obtained from NASA STI is fairly good, although it is not always possible to see the effects discussed in the text. No original paper copies of this report are known to the present author, so the original image quality is unknown. In nearly all cases, transition occurs after separation. When the nitrogen was cooled before being blown out of the model, transition occurred earlier. It appears that in some cases, transition occurred before separation, but these cases are not described clearly. In any case, since the model geometry is not documented, further analysis does not seem feasible unless additional reports describing these experiments can be located, as seems possible.

Laganelli et al. 1972-1975

Laganelli et al. first made a series of measurements at Mach 8.0 in AEDC Tunnel B with a 4-deg. half-angle sphere-cone model with provision for blowing through the nose only [49]. The model was 55.1 in. long with a 0.16-in. nose radius. The porous nose was 5.4 in. long, followed by an impervious frustum. Measurements were made with 14 pressure taps and 100 thermocouples. The freestream unit Reynolds number was 3.8×10^6/ft. and the angle of attack ranged from zero to 8 deg. Nitrogen was blown through the nose at rates of $\dot{m} = 0.015, 0.046,$ and 0.095, where $\dot{m}$ is the total massflow through the nose divided by the freestream massflow per unit area and the base area of the cone. At zero AOA, the boundary layer remained laminar to 66% of the cone length, whereas when $\dot{m} = 0.046$, transition moved upstream to about 18% of the length. At 1-deg. AOA, windward transition was similar with and without blowing, but leeside transition occurred much earlier when $\dot{m} = 0.046$. At higher AOA, blowing had less effect even on leeside transition. These effects appeared to be associated with the crossflow of low-momentum fluid from windward to leeward. The results at zero angle of attack should be compared to those of Starkenberg and Plostins, but this would require further analysis.

Laganelli et al. then made an extensive series of measurements with a complex blowing model in AEDC Tunnel B at Mach 8. Although the details only appear in limited-distribution reports, a summary was presented in Ref. [48]. The 5-deg. half-angle sharp cone had a nose radius of 0.002 inches. As shown in Fig. 11, it contained four separate chambers to permit axial variation of blowing rates. Mass was injected through the surface with uniform and non-uniform distributions, using air, helium, argon, and Freon, with rates of $\lambda_\infty = (\rho v)_w/(\rho u)_\infty = 0.0, 0.0005, 0.0025,$ and 0.0035, where $(\rho v)_w$ is the average massflow normal to the wall, and $(\rho u)_\infty$ is the freestream massflow per unit area. The first 9.47 inches of the cone was impervious. Measurements were made at angles of attack of 0, 3, 5, and 10 deg.,

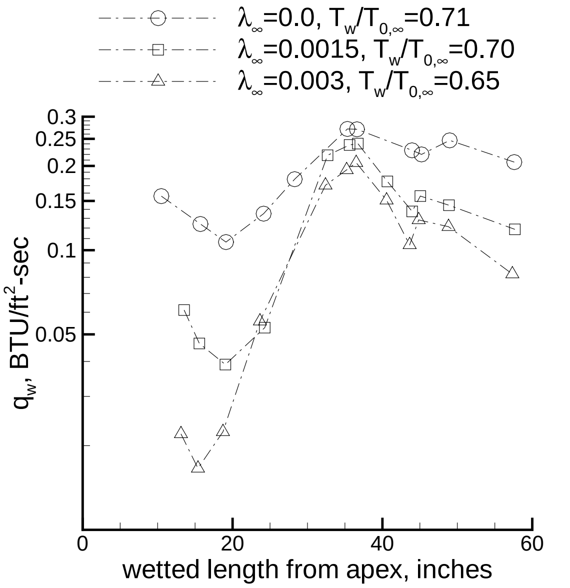

Figure 12: Effect of Mass Addition on Surface Heat Transfer. Equilibrium Wall Temperature. Redrawn from Ref. [48, Fig. 5a]

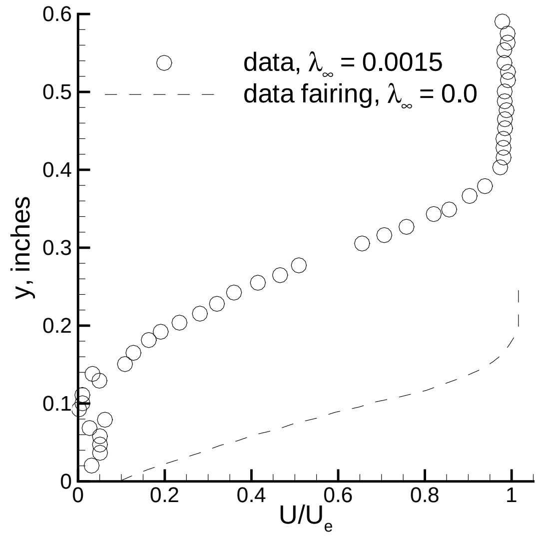

Figure 13: Velocity Profile Showing Effect of Mass Addition. Equilibrium Wall Temperature. Redrawn from Ref. [48, Fig. 9a]

at unit Reynolds numbers of $0.3 - 3.8 \times 10^6$/ft. Instrumentation included 26 heat-transfer gauges and 34 pressure taps. Boundary layer profiles included pitot pressure, total temperature, mass concentration, and static pressure. Surface data was obtained on a cold wall immediately after model injection, while both surface and profile data were obtained under hot-wall conditions after the model temperature reached equilibrium. Ref. [48] contains only a few samples of a large well-documented dataset.

Fig. 12 shows sample results for the heat-transfer distribution in the equilibrium-wall case with air injection. The angle of attack is zero, the freestream unit Reynolds number is 1.3×10^6/ft., and the freestream Mach number is 7.9. The lines are drawn only to aid the eye. The onset of transition, taken as the minimum in heat transfer, moves only slightly upstream as the blowing is turned on and increased. The end of transition, taken as the maximum in heat transfer, also moves only slightly when the blowing is varied. These results appear to contradict Fig. 4, perhaps because of the extensive impervious region at the cone tip. A detailed analysis would be required to understand the possible causes of the difference.

Fig. 13 shows a sample velocity profile in a region between the onset and end of transition, both with and without air injection. The profile was obtained 28 in. axially downstream of the nose. Here, y is the distance normal to the wall, U is the velocity parallel to the wall, and U_e is the velocity at the boundary-layer edge. The angle of attack is again zero, the freestream unit Reynolds number is 1.3×10^6/ft., and $M_\infty = 7.9$. The boundary layer thickens by more than a factor of two when blowing commences, and there is a large region of blown gas near the wall with very small velocity. There are 6 profiles shown in Ref. [48], for both velocity and total temperature, with many more presumably shown in the source documents. It would be very interesting to compare these profiles to a detailed computation.

Demetriades 1974

Demetriades shows data from Tunnel B on a nearly-sharp cone with blowing at zero and nonzero AOA [15]. Second-mode waves were observed under all these conditions, as described in the introduction, and shown in Figs 5 and 6. However, this short paper contains few details.

Summary

Ablation generates gas flow into the boundary layer from the wall. When this mass addition is simulated in wind tunnels and ballistic ranges, transition moves upstream. This upstream movement is generally larger for higher massflow rates and lighter gases. Blowing that occurs farther upstream generally appears to have a larger effect.

Blowing and ablation are only some of the many factors that affect transition. Simple algebraic parameters are not sufficient to capture the complex physics of the instability and transition process. It remains to be seen if reasonably simple semi-empirical stability-based methods such as e^N contain enough physics to capture the critical trends. The present review has identified a number of experimental datasets which should be compared to these modern stability-based transition-estimation methods.

Experimental data is more generally available for blowing-induced transition on slender cones near zero angle of attack. Laganelli et al. measured both transition and the boundary layer profiles, for example. However, there are no quantitative measurements of the instabilities that lead to transition, even for these geometries. Measurements on blunt bodies and models at large angle of attack are much more difficult, since the shock/boundary-layer interaction on the nozzle wall causes tunnel-starting difficulties that lead to requirements for large and expensive wind tunnels. Kaattari's measurements do provide a public-release dataset for comparing e^N methods to transition for a hemisphere, although he measured only transition and not the boundary layer profiles. Quantitative measurements of the instabilities leading to transition are again needed for blunt bodies.

Transition on bodies at angle of attack is much more complex, since the flow is now three-dimensional, introducing crossflow and the crossflow instability. Laganelli et al. also provide some initial data to evaluate blowing effects on a slender cone under these conditions. However, much more experimental data is needed for these flows, including again measurements of the instabilities that may occur and of the effect of blowing on these instabilities.

Acknowledgements

This review originated in work supported by Northrop-Grumman as part of the Orion program. It was continued with support from NASA Johnson and the NASA Constellation University Institutes Project. The author's research has also been funded by AFOSR and Sandia National Laboratories. A number of people suggested various references over many years, including Dick Batt of TRW, Tony Martellucci of SAIC, and Tom Horvath of NASA Langley. Joe Marvin of NASA Ames, Peter Ploskins of ARL, John Bertin of Rice Univ., and Robert Feldhuhn of NOL provided additional information regarding their research.

References

[1] Steven P. Schneider. Laminar-turbulent transition on reentry capsules and planetary probes. *Journal of Spacecraft and Rockets*, 43(6):1153–1173, Nov.-Dec. 2006. See erratum with correct color figures, v. 44, no. 2, pp. 464-484, March-April 2007.

[2] Steven P. Schneider. Flight data for boundary-layer transition at hypersonic and supersonic speeds. *Journal of Spacecraft and Rockets*, 36(1):8–20, 1999.

[3] Steven P. Schneider. Effects of high-speed tunnel noise on laminar-turbulent transition. *Journal of Spacecraft and Rockets*, 38(3):323–333, May–June 2001.

[4] Steven P. Schneider. Hypersonic laminar-turbulent transition on circular cones and scramjet forebodies. *Progress in Aerospace Sciences*, 40(1-2):1–50, 2004.

[5] Steven P. Schneider. Effects of roughness on hypersonic boundary-layer transition. *Journal of Spacecraft and Rockets*, 45(2):193–209, Mar.-Apr. 2008.

[6] Steven P. Schneider. Hypersonic boundary-layer transition on blunt bodies with roughness. Paper 2008-0501, AIAA, January 2008. Revised version submitted to the J. Spacecraft and Rockets.

[7] Mark V. Morkovin. Critical evaluation of transition from laminar to turbulent shear layers with emphasis on hypersonically traveling bodies. Technical Report AFFDL-TR-68-149, Air Force Flight Dynamics Laboratory, March 1969. DTIC citation AD-686178.

[8] John O. Powers, Gerhard Heiche, and S.F. Shen. The stability of selected boundary-layer profiles. Technical Report NOL-TR-62-143, Naval Ordnance Laboratory, April 1963. Citation AD0406188 in DTIC.

[9] J. O. Powers. Formulation of the complete equations of boundary layer stability with mass transfer. Technical Report NOL-TR-66-187, Naval Ordnance Laboratory, October 1966. Citation AD0644532 in DTIC.

[10] Charles J. Scott and Gerald E. Anderson. Boundary-layer transition with gas injection. *J. of the Aerospace Sciences*, 25(12):791, December 1958.

[11] C.C. Pappas and A. Okuno. Heat-transfer measurement for binary gas laminar boundary layers with high rates of injection. Technical Report NASA TN-D-2473, NASA, Sept. 1964.

[12] C.C. Pappas and George Lee. Heat transfer and pressure on a hypersonic blunt cone with mass addition. *AIAA Journal*, 8(5):954–956, May 1970.

[13] C. C. Pappas. The effect of injection of foreign gases on skin friction of the turbulent boundary layer. In *NACA Conference on High-Speed Aerodynamics*, pages 245–252, March 1958. Paper is NASA citation 71N75303, conference is citation 71N75285, NASA-TM-X-67369.

[14] C. Pappas and A. Okuno. Measurements of skin friction of the compressible turbulent boundary layer on a cone with foreign gas injection. *J. Aero. Sci.*, 27:321–333, May 1960. See also AIAA Paper 69-716.

[15] A. Demetriades. Hypersonic viscous flow over a slender cone, part III: laminar instability and transition. Paper 74-535, AIAA, June 1974.

[16] H.M. McMahon. An experimental study of the effect of mass injection at the stagnation point of a blunt body. Hypersonic Project Memorandum 42, Guggenheim Aeronatical Laboratory, California Institute of Technology, May 1958.

[17] Max Wilkins and Michael E. Tauber. Boundary-layer transition on ablating cones at speeds to 7 km/s. Paper 66-27, AIAA, January 1966. See also AIAA J., v. 6, pp. 174-175, Jan. 1968.

[18] Max E. Wilkins and Gary T. Chapman. Free flight determination of boundary layer transition on small scale cones in the presence of surface ablation. In W.D. McCauley, editor, *Proceedings of the boundary layer transition workshop held 3-5 November 1971*, pages 3–1 to 3–21, 1971. Aerospace Report TOR-0172(S2816-16)-5, DTIC citation AD909223. See also NASA-TM-X-68867, Aug. 1972.

[19] A. Demetriades, A.J. Laderman, L. Von Seggern, A. T. Hopkins, and J. C. Donaldson. Effect of mass addition on the boundary layer of a hemisphere at Mach 6. *J. of Spacecraft and Rockets*, 13(8):508–509, August 1976.

[20] R.H. Feldhuhn. Heat transfer from a turbulent boundary layer on a porous hemisphere. Paper 76-119, AIAA, January 1976.

[21] R.R. Williams, J.W. Stultz, and W.A. Rinehart. Nosetip boundary layer transition investigation using a pressure ramp technique in an arc heater facility. In *Proceedings of the 22nd International Instrumentation Symposium held May 25-27, 1976, Anaheim, California*, pages 1–8, May 1976.

[22] Daniel C. Reda. Comparative transition performance of several nosetip materials at defined by ballistics-range testing. In *Proceedings of the 25th International Instrumentation Symposium held May 7-10, 1979, Anaheim, California*, pages 89–104, May 1979. See also the journal version in ISA Transactions, vol. 19, no. 1, Jan. 1980, pp. 83-98.

[23] George E. Kaattari. Effects of mass addition on blunt-body boundary-layer transition and heat transfer. Technical Report NASA-TP-1139, NASA, January 1978.

[24] E.M. Winkler, M.T. Madden, R.L. Humphrey, and J.A. Koenig. Supersonic ablation studies with Teflon. Technical Report NOL-TR-69-125, Naval Ordnance Laboratory, October 1969. Citation AD699889 in DTIC.

[25] R.L. Baker. Low temperature ablator nosetip shape change at angle of attack. Paper 72-0090, AIAA, January 1972.

[26] Chul Park. Injection-induced turbulence in stagnation-point boundary layers. *AIAA Journal*, 22(2):219–225, February 1984.

[27] T. Yamada, H. Ogawa, S. Nonaka, Y. Inatani, K. Nakakita, and T. Yamazaki. An experimental study on the boundary layer transition due to gas injection from capsule-shape body surface. Technical Report SP-17, Japanese Institute of Space and Astronautical Science, March 2003. NASA citation 20040003942. In English.

[28] C.J. Scott. Experimental investigation of laminar heat transfer and transition with foreign gas injection on a 16-deg. porous cone at Mach 5. Technical Report AFOSR-TN-60-1370, University of Minnesota, October 1960. DTIC citation AD258009. Rosemount Aeronautical Laboratories Research Report No. 174.

[29] James C. Dunavant and Philip E. Everhart. Exploratory heat-transfer measurements at Mach 10 on a 7.5-deg. total-angle cone downstream of a region of air and helium transpiration cooling. Technical Note TN-D-5554, NASA, December 1969.

[30] G. G. Mateer and H.K. Larson. Unusual boundary-layer transition results on cones in hypersonic flow. *AIAA Journal*, 7(4):660–664, April 1969.

[31] V. DiCristina. Three-dimensional laminar boundary-layer transition on a sharp 8-deg. cone at Mach 10. *AIAA Journal*, 8(5):852–856, May 1970.

[32] Michael C. Fischer. An experimental investigation of boundary-layer transition on a 10-deg. half-angle cone at Mach 6.9. Technical Report NASA TN-D-5766, NASA, April 1970.

[33] M.C. Fischer. Hypersonic boundary-layer transition on ablating and nonablating cones. *AIAA Journal*, 7(10):2037–2038, October 1969.

[34] J.J. Ginoux. *Streamwise Vortices in Laminar Flow*, pages 395–422. AGARD, 1965. AGARDograph 97.

[35] Joseph G. Marvin and Clifford M. Akin. Combined effects of mass addition and nose bluntness on boundary-layer transition. *AIAA Journal*, 8(5):857–863, May 1970.

[36] C.R. Wimberly, F.K. McGinnis, and J.J. Bertin. Transpiration and film cooling effects for a slender cone in hypersonic flow. *AIAA Journal*, 8(6):1032–1038, June 1970.

[37] C.J. Stalmach, Jr., J.J. Bertin, T.C. Pope, and M.H. McCloskey. A study of boundary layer transition on outgassing cones in hypersonic flow. Technical Report NASA-CR-1908, NASA, December 1971.

[38] Anthony Martellucci. Effects of mass transfer on hypersonic turbulent boundary-layer properties. *AIAA Journal*, 10(2):181–187, February 1972.

[39] A. Martellucci. Effects of mass transfer on hypersonic turbulent boundary layer properties. Paper 72-184, AIAA, January 1972.

[40] A. Martellucci and H. Rie. Effects of mass addition on viscous flow parameters. Technical Report TR-71-60, SAMSO, January 1971. DTIC citation AD0724188.

[41] John Starkenberg and R.J. Cresci. Boundary layer transition on a film cooled slender cone. *AIAA Journal*, 14(4):461–467, April 1976.

[42] P. Plostins and R.J. Cresci. Effects of mass transfer on transition behavior at high speeds. M/AE Report 82-9, Brooklyn Polytechnic, June 1982.

[43] Peter Plostins. *A theoretical and experimental investigation of the hypersonic viscous shock layer for large rates of injection*. PhD thesis, Polytechnic Institute of New York, Dept. of Aerospace Engineering and Applied Mechanics, June 1981.

[44] A.H. Boudreau. Transition measurements via heat-transfer instrumentation on a 0.5 bluntness 9.75-deg. cone at Mach 7 with and without mass addition. Paper 85-1004, AIAA, June 1985.

[45] A.H. Boudreau. Transition measurements via heat-transfer instrumentation on a 0.5 bluntness 9.75-deg. cone at Mach 7 with and without mass addition. Technical Report AEDC-TR-77-86, Arnold Engineering Development Center, September 1977. DTIC Citation ADB021861. Approved for public release, Mar. 1984.

[46] William J. Yanta, Arnold S. Collier, and Timothy S. Smith. Measurements of a supersonic turbulent boundary layer with mass addition. Paper 89-0135, AIAA, January 1989.

[47] Mark V. Morkovin and John C. Donohoe. Exploratory investigations of the effects of gas injection through a porous model on separation, transition, static stability and control effectiveness of a blunt entry body at Mach number 7.3. Technical Report ER-14607, Martin Marietta Corporation, July 1967. NASA-CR-73121.

[48] A.L. Laganelli, R.P. Fogaroli, and A. Martellucci. The effects of mass transfer and angle of attack on hypersonic turbulent boundary layer characteristics. Technical Report TR-75-35, AFFDL, April 1975. DTIC citation ADA012700.

[49] A.L. Laganelli and A. Martelluci. Downstream effects of gaseous injection through a porous nose. Paper 72-185, AIAA, January 1972.